

This is the final draft of the contribution published as:

Liu, Y., Wu, L., Kohli, P., Kumar, R., Stryhanyuk, H., Nijenhuis, I., Lal, R. (2019):
Enantiomer and carbon isotope fractionation of α -hexachlorocyclohexane by *Sphingobium indicum* strain B90A and the corresponding enzymes
Environ. Sci. Technol. **53** (15), 8715 – 8724

The publisher's version is available at:

<http://dx.doi.org/10.1021/acs.est.9b01233>

1 Enantiomer and Carbon Isotope Fractionation of α -Hexachlorocyclohexane by *Sphingobium*

2 *indicum* Strain B90A and the Corresponding Enzymes

3 Yaqing Liu,¹ Langping Wu,^{1,#} Puneet Kohli,² Roshan Kumar,² Hryhoriy Stryhanyuk,¹ Ivonne

4 Nijenhuis,¹ Rup Lal,² Hans-Hermann Richnow^{1,*}

5 ¹Department of Isotope Biogeochemistry, Helmholtz Centre for Environmental Research-UFZ,

6 Permoserstraße 15, 04318 Leipzig, Germany

7 ²Molecular Biology Laboratory, Department of Zoology, University of Delhi, Delhi-110007,

8 India

9 [#]Present address: Departments of Civil & Mineral Engineering, University of Toronto, 35 St.

10 George Street, Toronto, ON M5S 1A4, Canada

11

12 *Corresponding author: Hans-Hermann Richnow

13

14

15

16

17

18

19

20

21

22

23

24

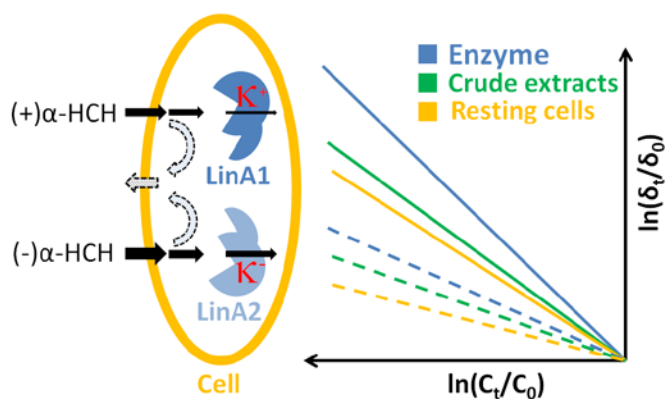
25

26

27

28 **ABSTRACT**

29 Chiral organic contaminants, like α -hexachlorocyclohexane (α -HCH), showed isotope
30 fractionation and enantiomer fractionation during biodegradation. This study aims to understand
31 the correlation between these two processes. Initial tests of α -HCH degradation by six
32 *Sphingobium* strains (with different LinA variants) were conducted. Results showed variable
33 enantiomer selectivity over the time course. In contrast, constant enantiomer selectivity was
34 observed in experiments employing (i) cell suspensions, (ii) crude extracts, or (iii) LinA1 and
35 LinA2 enzymes of strain B90A for α -HCH degradation in enzyme activity assay buffer. The
36 average value of enantioselectivity (ES) were -0.45 ± 0.03 (cell suspension), -0.60 ± 0.05 (crude
37 extract) and 1 (LinA1) or -1 (LinA2). The average carbon isotope enrichment factors (ϵ_c) of
38 (+) α - and (-) α -HCH were increased from cells suspensions ($-6.3 \pm 0.1\text{‰}$ and $-2.3 \pm 0.03\text{‰}$) over
39 crude extracts ($-7.7 \pm 0.4\text{‰}$ and $-3.4 \pm 0.02\text{‰}$) to purified enzymes ($-11.1 \pm 0.3\text{‰}$ and $-3.8 \pm$
40 0.2‰). The variability of ES and the ϵ_c were discussed based on the effect of mass transport and
41 degradation rates. Our study demonstrates that enantiomer and isotope fractionation of α -HCH
42 are two independent processes and both are affected by reactions of individual enzymes and
43 mass transport to a different extent.



44
45 **For TOC only**

46 INTRODUCTION

47 An increasing number of anthropogenic chemicals are chiral compounds which raise not only
48 environmental concerns but also possess enantiomer-specific environmental toxicity.¹ Estimates
49 suggest that up to one-third of all anthropogenic compounds such as fungicides, herbicides, and
50 antibiotics are chiral, of which many are produced by chemical synthesis as racemates.² Due to
51 the identical physical and chemical properties of enantiomers, the abiotic degradation is
52 identical for both the enantiomers.³ However, certain microorganisms preferably biodegrade one
53 enantiomer at higher rate leading to enantiomer fractionation i.e., a change in enantiomer ratios.
54 Enantioselectivity can be the result of the preferential uptake or selectivity of enzyme
55 catalysis.⁴ The changes in enantiomer ratios have been suggested as an indicator for
56 biodegradation of chiral compounds and have been applied to track *in situ* degradation at field
57 sites.^{5, 6} For evaluation of degradation at a field site, another well-developed method to assess
58 contaminants degradation at field sites is compound specific stable isotope analysis (CSIA).⁷⁻⁹
59 During the degradation of organic compounds, slightly different reaction rates of lighter and
60 heavier isotopologues can lead to the change of isotope composition in the substrate, known as
61 isotope fractionation.

62 The Rayleigh equation is extensively applied for the quantification of isotope fractionation.¹⁰
63 For the quantification of enantiomer fractionation, the Rayleigh equations (both simplified and
64 general forms) and enantioselectivity (ES) were applied in previous studies.¹¹⁻¹³ Both
65 enantiomer and isotope fractionation can be observed during the biodegradation due to different
66 reaction rates of enantiomers and isotopologues, respectively, and both were proposed for the
67 evaluations of biodegradation. However, it has not been fully evaluated yet how enantiomer and
68 isotope fractionation are linked and whether or not they are two independent processes.

69 α -Hexachlorocyclohexane (HCH) is one of the persistent organic pollutants appearing
70 worldwide as point source or dispersed pollution.¹⁴ The genes responsible for HCH aerobic
71 degradation, known as *lin* genes, are generally present in aerobic HCH degrader
72 *Sphingomonads*. These genes were first identified and characterized in *Sphingobium japonicum*

73 UT26,¹⁵ followed by *S. indicum* B90A.¹⁶ The product of this gene containing 156-amino acids is
74 known as the HCH dehydrochlorinase and was localized in the periplasm.¹⁵ The LinA enzyme
75 catalyzes the initial step of dehydrochlorination, converting α -HCH into β -
76 pentachlorocyclohexene (β -PCCH).¹⁷ It has been reported that the *linA* genes are under
77 continuous selection pressure and thus exist in several variants.¹⁸⁻²² There are two copies of *linA*
78 genes *i.e.*, *linA1* and *linA2* present in *S. indicum* B90A and *Pseudomonas aeruginosa* ITRC-5,
79 whereas only *linA2* is present in *S.indicum* UT26.²³ The *linA1* and *linA2* genes of strain B90A
80 differ by 10% in their amino acid sequence, and the corresponding enzymes preferentially
81 degrade (+) α -HCH and (-) α -HCH enantiomers, respectively.²⁴⁻²⁶ The degradation of individual
82 α -HCH enantiomers by these sphingomonads involves different enzymes (LinA1 and LinA2),
83 and the expression of the enzymes may not be stable during growth which may affect the
84 enantiomer preference and lead to variable enantiomer fractionation. In this case, employing cell
85 suspensions without nutrients (prevent growth and synthesis of biomass) as well as crude
86 extracts of these cells for the degradation of α -HCH should lead to stable enantiomer preference
87 and the enantiomer fractionation can be characterized. Further, activity assays with LinA1 and
88 LinA2 enzymes (separately expressed as functional S-glutathione transferase (GST) fusion
89 proteins and enabling the catalysis of α -HCH enantiomers separately) allow a better
90 understanding of the enantiomer fractionation as well as isotope fractionation.

91 In this study, the initial set of experiments involving six *Sphingobium* strains (namely
92 *Sphingobium quisquiliarum* P25, *S. lucknowense* F2, *S. chinhatense* IP26, *S. ummariense* RL3,
93 *Sphingobium sp.* HDIPO4, *S. baderi* LLO3) were conducted in growth medium to investigate
94 the enantiomer preference during α -HCH degradation. Furthermore, in order to characterize the
95 contributions of substrate uptake, mass transport and enzymatic reactions on the observable
96 isotope and enantiomer fractionation, four sets of degradation experiments using cell
97 suspensions, crude extracts, LinA1 and LinA2 were conducted in buffer. With the objective to
98 investigate the correlation of isotope and enantiomer fractionation processes, the obtained

99 isotope and enantiomer fractionation were discussed based on (1) mass transfer: The effect of
100 membrane was discussed by comparing the degradation in cell suspension and crude extract; the
101 effect of vesicles was discussed by comparing the crude extract and purified enzymes and (2)
102 degradation rates: The ES and ϵ_c values were compared in each set of experiments based on the
103 reaction kinetics.

104 **MATERIALS AND METHODS**

105 **Chemicals.** α -HCH (analytical purity, 99%), hexachlorobenzene (HCB, analytical purity, 97%),
106 imidazole (analytical purity, 99%) and ampicillin (analytical purity, 95%) were purchased from
107 Sigma Aldrich (Germany). *n*-pentane (analytical purity, 99%) was supplied by Carl Roth,
108 Germany. TRIS was supplied by Geyer, Germany.

109 **Bacterial Strains and Cultivation Conditions.** *Sphingobium spp.* (strain B90A, P25, F2, IP26,
110 RL3, HDIPO4, LLO3) and *E.coli* BL21 (AI) were maintained in the Molecular Biology
111 Laboratory, University of Delhi, India. The information for cultivation is provided in the
112 Supporting Information (SI) section 1.

113 **Cell Suspension and Bacterial Crude Extracts of B90A.** Bacterial cells were grown in LB
114 medium until the A_{600} of cultures reached 0.5-0.6 (logarithmic phase). The cells were harvested
115 by centrifugation at $8000 \times g$ at 4 °C for 20 min to obtain a cell pellet. The pellet was washed
116 twice by sequential re-suspension and centrifugation with 0.1 M TRIS-HCl buffer at pH 7.5 to
117 remove nutrients and substrates for growth. Subsequent degradation experiments were
118 completed within several hours after the cell suspensions were prepared. The bacterial pellet
119 was stored at -20 °C, and the crude extracts were prepared with a French Press (Thermo Fisher
120 Scientific, Bremen) at 20.000 psi before usage.

121 **Enzyme Expression and Purification.** The *E. coli* cells carrying the *linA1* and *linA2* genes,
122 respectively, were grown overnight before inoculation (1% v/v) in 100 mL LB media (See SI)
123 amended with antibiotics. Cultures were incubated at 30°C while shaking at 200 rpm until the
124 OD_{600} reached 0.5-0.6 and induced with L-(+)-arabinose (see SI). The cells were then harvested

125 by centrifugation at $8000 \times g$ for 15 min at 4 °C. Enzyme purification procedures are provided in
126 the SI section 2.

127 **Degradation Experiments.** In all the degradation experiments, the initial concentration of α -
128 HCH was 5.5 μM (each bottle was spiked 5.5 μL of stock solution with the concentration of
129 0.1M in acetone). For each set of experiments, two abiotic controls without adding biomass
130 were performed and treated identically until extraction. All bottles were incubated at 30 °C in a
131 shaking incubator (200 rpm). The sampling and extraction were done as reported elsewhere.²⁷

132 Degradation experiments with growing cells: (1) Degradation of α -HCH by six *Sphingobium*
133 spp.(strain P25, F2, IP26, RL3, HDIPO4, LLO3) were conducted in 240 mL bottles filled with
134 100 mL mineral salt medium with glucose as the carbon source (SI section 1). (2) Degradation
135 experiment using strain HDIPO4 under nutrient-limited condition by reducing the glucose to 1%
136 was compared to the amount used experiments (1) but other conditions are the same.

137 Batch experiments with cell suspensions, crude extracts and purified enzymes were performed
138 in 240 mL bottles filled with 100mL Tris-buffer (0.1 M, pH = 7.5). (1) Degradation experiments
139 with cells suspensions: different volumes of cell suspensions with a cell density of $2.5\text{-}3.0 \times 10^8$
140 cells mL^{-1} were used for four sets of experiments, labeled as a (500 μL), b (200 μL), c (100 μL),
141 d (50 μL). (2) Degradation experiments with crude extracts: different amounts of crude extracts
142 (obtained from the cell suspension with the cell density of $2.5\text{-}3.0 \times 10^8$ cells mL^{-1}) were used for
143 four sets of experiments, labeled as e (200 μL), f (100 μL), g (50 μL), h (50 μL , a replicate of
144 experiment g). (3) Degradation experiments with LinA2 enzyme: three sets of degradation
145 experiments were conducted by using different amounts of LinA2 enzyme (240 ng μL^{-1}),
146 labeled as i (10 μL), j (8 μL), k (5 μL). (4) Degradation experiments with LinA1 enzyme: two
147 sets of experiments were conducted by using different amounts of LinA1 enzyme (70 ng μL^{-1}),
148 labeled as l (10 μL) and m (5 μL).

149 **Analytical Methods and Data Evaluation.** The concentration of HCH was analyzed by an
150 Agilent 6890 series GC (Agilent Technologies, USA) equipped with a FID (SI section 3). The

151 concentration of protein was quantified by NanoDrop ND-1000 Spectrophotometer from
152 Thermo Fisher Scientific. The carbon isotope composition was analyzed by a gas
153 chromatography isotope ratio mass spectrometer (GC-IRMS), as described previously.²⁸

154 Enantiomer fraction (EF) is applied for explaining the relationship between different
155 enantiomers. The EF(-) is calculated as $A^-/(A^++A^-)$ and $EF(+)=A^+/(A^++A^-)$, where A^+ and A^-
156 correspond to the peak areas or concentrations of (+) and (-) enantiomers. An $EF(-) > 0.5$ shows
157 the preferential degradation of (+) enantiomer, and an $EF(-) < 0.5$ indicates the preferential
158 degradation of (-) enantiomer.

159 Enzymatic reactions are frequently described by the Michaelis-Menten kinetics as showed in
160 equation 1.

$$161 \quad v = k_{cat} \cdot [E]_0 \frac{[S]}{k_M + [S]} \quad (1)$$

162 Where v , k_{cat} , $[E]_0$, $[S]$ and K_M are the reaction rate, turnover number, initial enzyme
163 concentration, substrate concentration and Michaelis constant, respectively. The condition $[S]$
164 $\ll K_M$ can be assumed as even lower substrate concentration (2.5 μ M for each α -HCH
165 enantiomer) applied in this study compare to the previous report.²⁹ And equation 1 then can be
166 modified to equation 2 and applied for evaluating the degradation kinetics of α -HCH
167 enantiomers by cell suspensions, crude extract and enzymes in this study.

$$168 \quad v = -\kappa \cdot [S] \quad (2)$$

169 Where $\kappa = -\frac{k_{cat} \cdot [E]_0}{k_M}$ is the first order rate constants of the reaction.

170 For the evaluation of enantiomer fractionation, the excess of the degradation rates for (+) α -HCH
171 over the (-) α -HCH was used to define the ES which was quantified by the following equation.^{4,}

172 ³⁰⁻³²

$$173 \quad ES = \frac{\kappa^+ - \kappa^-}{\kappa^+ + \kappa^-} \quad (3)$$

174 Where κ^+ and κ^- are the first order rate constants for the degradation of (+) α -HCH and (-) α -HCH,
175 respectively. When the enantiomers are degraded equally ($\kappa^+ = \kappa^-$), no enantiomer selective

176 degradation will be observed and ES=0. If only one enantiomer is degraded, then ES=1 (κ^- =0,
177 only (+) α -HCH is degraded) or ES=-1 (κ^+ =0, only (-) α -HCH is degraded).
178 The simplified Rayleigh equation in logarithmic form was used to quantify the stable carbon
179 isotope fractionation of the biodegradation process in this study. The carbon isotope enrichment
180 factor (ϵ_c) was determined using equation 4.

$$181 \quad \ln\left(\frac{(\delta_t^{13}C+1)}{\delta_0^{13}C+1}\right) = \epsilon_c \ln\left(\frac{C_t}{C_0}\right) \quad (4)$$

182 ϵ_c was reported in per mil and derived from the slope of the linear regression of $\ln(C_t/C_0)$ vs
183 $\ln[(\delta_t^{13}C+1)/(\delta_0^{13}C+1)]$. The error of ϵ_c was reported as the 95% confidence interval (CI)
184 determined by regression analysis.¹²

185 The apparent kinetic isotope effect was calculated as previously described using equation 5.³³

$$186 \quad AKIE_C = \frac{1}{1 + \frac{nz}{x} * \epsilon_c / 1000} \quad (5)$$

187 Where n is the total number of carbon atoms in a molecule, x is the number of atoms at reactive
188 positions, and z is the number of indistinguishable reactive positions for intramolecular
189 competition.

190 **RESULTS**

191 **Degradation by Growing Cells.** In experiment (1), carbon isotope enrichment of α -HCH
192 enantiomers associated with enantiomer preferential degradation was observed in growing cells
193 experiments (except the controls) (Figure S1). This result indicates that the enantiomer and
194 isotope fractionation potentially can be used for the quantification of α -HCH biodegradation.
195 Plotting the enantiomer fraction (EF) of (-) α -HCH over time, the EF(-) was varied from 0.50 up
196 to 0.59 during the degradation period (Figure S2). Each of the *Sphingomonas* species has at least
197 two enzymes (LinA1 and LinA2) catalyzing the initial step of α -HCH enantiomer degradation.
198 Thus, we speculated that the expression of LinA enzymes changed during growth, which might
199 affect the degradation kinetics of individual enantiomers and therefore the enantiomer

200 preference changed. In experiment (2), the result shows that the growing culture performed a
201 constant enantiomer preference under nutrient-limited condition (Figure S3).

202 Due to the possibility of variable isotope and enantiomer fractionation under the growth
203 condition, experiments in buffer which do not contain the necessary nutrients for growth were
204 conducted with cell suspensions, crude extracts and purified enzymes. The pseudo-first order
205 kinetic rate constants (κ), ϵ_c and the ES values obtained from these experiments are summarized
206 in Table 1. In all the abiotic controls, both the concentration and the isotope composition are
207 remain constant until the end of the experiments indicating that no other processes affect the
208 biodegradation in this study.

209 **Degradation by Cell Suspensions.** The degradation of both enantiomers could be described by
210 pseudo-first order kinetics, which indicates that the ratio of LinA enzymes and their activities
211 were constant over the course of the individual degradation experiments (experiment a-d). The
212 relatively short experimental time (1.5h to 5h, Figure S4) and the absence of growth substrates
213 and nutrients preclude growth and significant *de novo* synthesis of enzymes unlikely. Thus, the
214 enzyme inventory is assumed to be constant. For (+) α -HCH transformation, different κ^+ values
215 were observed: $0.49 \pm 0.03 \text{ h}^{-1}$, $0.30 \pm 0.03 \text{ h}^{-1}$, $0.12 \pm 0.02 \text{ h}^{-1}$ and $0.06 \pm 0.01 \text{ h}^{-1}$ (Figure 1, a-d).
216 The obtained ϵ_c^+ in experiment a-d ($-6.4 \pm 0.7\%$, $-6.2 \pm 1.2\%$, $-6.1 \pm 1.1\%$ and $-6.1 \pm 1.4\%$,
217 respectively; Table 1 and figure 2, a-d) were statistically identical and thus described the isotope
218 fractionation of (+) α -HCH robustly. For (-) α -HCH transformation, no consistent isotope
219 enrichment which can be quantified by Rayleigh equation was observed at higher κ^- values of
220 $0.81 \pm 0.12 \text{ h}^{-1}$ and $0.76 \pm 0.09 \text{ h}^{-1}$ (FigureS3 a, b). However, at lower rates of $\kappa^- = 0.35 \pm 0.02 \text{ h}^{-1}$ and
221 $0.15 \pm 0.02 \text{ h}^{-1}$ (experiment c and d, Figure 1 and Table 1), significant isotope enrichment was
222 observed with $\epsilon_c^- = -2.3 \pm 0.4\%$ and $-2.3 \pm 0.3\%$ (Figure 2 and Table 1), respectively. The
223 relatively higher transformation rates in experiment a and b lead to the non-observable carbon
224 isotope fractionation in both experiments, which suggests masking of isotope fractionation by
225 the rate limiting step prior to the isotope sensitive bond cleavage. At higher degradation rates,

226 the ES value was only reduced in the experiment a (-0.25 ± 0.08) whereas the ES values of -
227 0.43 ± 0.06 , -0.49 ± 0.07 and -0.43 ± 0.09 in experiment b-d are similar (Table 1).

228 **Degradation by Crude Extracts.** The degradation of α -HCH enantiomers by using different
229 amounts of crude cell extracts followed first-order kinetics (Figure 1, experiment e-h).
230 Significant and identical ϵ_c^+ were obtained as $-7.4\pm 0.7\%$ and $-8.0\pm 1.3\%$ (experiment e and f,
231 Figure 2 and Table 1) during (+) α -HCH transformation when the κ^+ values were $0.30\pm 0.07\text{ h}^{-1}$
232 and $0.12\pm 0.02\text{ h}^{-1}$, respectively. In the case of (-) α -HCH transformation, no significant isotope
233 enrichment (Figure S5 e) was observed when the corresponding κ^- values were $0.58\pm 0.13\text{ h}^{-1}$
234 (experiment e, Figure 1 and Table 1). When the κ^- value was $0.45\pm 0.06\text{ h}^{-1}$ (experiment f,
235 Figure 1 and Table 1), a relatively smaller ϵ_c^- ($-1.9\pm 0.4\%$) was obtained compare to the ϵ_c^-
236 values ($-3.4\pm 0.5\%$ and $-3.4\pm 0.6\%$ for experiment g and h, Figure 2 and Table 1) which were
237 obtained at lower reaction rates ($0.19\pm 0.02\text{ h}^{-1}$ and $0.18\pm 0.02\text{ h}^{-1}$). At higher transformation rates
238 the isotope fractionation of (-) α -HCH was low or could not be observed compared to isotope
239 fractionation at lower degradation rates, which is similar with the observation in the experiments
240 with cell suspensions. In contrast, only the ES value of -0.32 ± 0.15 from experiment e was
241 relatively lower compared to that of -0.57 ± 0.07 , -0.65 ± 0.08 and -0.57 ± 0.10 (Table 1) from
242 experiment f, g and h, respectively.

243 **Degradation by Purified Enzymes.** The enzyme experiments showed a nearly exclusive
244 degradation of (-) α -HCH by LinA2 and (+) α -HCH by LinA1. The degradation of α -HCH
245 enantiomers was investigated by using different amounts of purified enzymes and could be
246 described by the first-order kinetics. LinA1 degraded preferentially (+) α -HCH with a κ^+ of
247 $0.28\pm 0.02\text{ h}^{-1}$ and $0.13\pm 0.02\text{ h}^{-1}$ (experiment l and m, Figure 1, Table 1) and the obtained
248 ϵ_c^+ values were $-11.3\pm 2.0\%$ and $-10.9\pm 1.5\%$ (Figure 2, Table 1). (-) α -HCH degradation by
249 LinA2 resulted in a κ^- of $0.65\pm 0.10\text{ h}^{-1}$, $0.54\pm 0.28\text{ h}^{-1}$ and $0.27\pm 0.05\text{ h}^{-1}$ (experiment i-k, Figure
250 1, Table 1), and the corresponding ϵ_c^- were $-3.7\pm 0.6\%$, $-4.0\pm 1.0\%$ and $-3.6\pm 0.5\%$, respectively.

251 Since LinA1 and LinA2 showed nearly exclusive enantiomer preference of (+) α -HCH and (-) α -
252 HCH, the calculated ES values from LinA1 and LinA2 experiments were 1 and -1, respectively.

253 **DISCUSSION**

254 **Variability of Enantiomer Fractionation.** High variability of enantiomer fractionation was
255 observed during α -HCH degradation by the six *Sphingobium* strains in growing cell experiment
256 (1). This indicates that the degradation rates of the enantiomers were not constant during the
257 whole process, which suggests changes in the abundance of LinA1 and LinA2 enzymes during
258 growth may lead to preferential degradation of individual α -HCH enantiomers over the course
259 of the experiment. However, the stable enantiomer preference in growing cell experiment (2)
260 indicates that the expression of enzymes may relatively slow in nutrient-limited condition. In
261 addition, the enantiomer selectivity of *S. indicum* B90A observed in different studies also
262 indicates the variability of enantiomer fractionation. For example, biodegradation of α -HCH by
263 *S.indicum* B90A showed preferential degradation of the (-) α -HCH enantiomer at the beginning
264 of the degradation and later changed to (+) α -HCH.¹² However, enantioselectivity of α -HCH was
265 not observed with the same strain elsewhere.³² In the present study, the cell suspensions and
266 crude extracts both preferred (-) α -HCH transformation. This indicates that different growth
267 phases (lag phase, log phase, and stationary phase) or different cultivation conditions lead to
268 changes in the regulation of the LinA1 and LinA2 abundance. This is in agreement with the
269 variable enantiomer selectivity of the six *Sphingobium* strains. Thus, different ratios of LinA1
270 and LinA2 may be expressed under different growth conditions which change the selectivity of
271 enantiomer degradation.

272 **Relationship between Isotope and Enantiomer Fractionation.** Isotope fractionation is
273 determined by bond cleavage or formation in the first irreversible reaction step and can be
274 modified due to rate limitation of preceding steps in a complex biochemical reaction.^{34, 35} The
275 observed isotope fractionation contains information on the transition state of bond cleavage and
276 kinetic rate limitation prior to irreversible bond cleavage. Isotope fractionation depends on the

277 kinetics of bond cleavage in the transition state which can be quantified by the Rayleigh
278 equation (equation 4). For the degradation of α -HCH, LinA dehydrochlorinates the substrates
279 most likely via an E2 elimination,³⁶ which is probably identical for both enantiomers.³⁷ In this
280 study, an elimination reaction with concerted bond cleavage at two axial H/Cl pairs of α -HCH to
281 form pentacyclohexenes (1,3S,4S,5R,6S-PCCH for (+) α -HCH and 1,3R,4R,5S,6R-PCCH for (-
282) α -HCH) during dehydrochlorination was assumed as in a previous study.³⁸ In this case, four
283 carbons with axial chlorine hydrogen pairs ($x=4$) with two indistinguishable positions ($z=2$)
284 were involved in the reaction. The calculated apparent kinetic carbon isotope effect (AKIE_C)
285 yields an average value of 1.035 ± 0.004 for LinA1 and 1.011 ± 0.001 for LinA2 (SI section 7,
286 Table S1). In the quantum chemical modelling study by Manna and Dybala-Defratyka, the
287 position-specific primary KIE_C values of (+) α -HCH dehydrochlorination are 1.0168 and 1.0218
288 for the C-H and C-Cl bond cleavage reaction, respectively, whereas the dehydrochlorination of
289 (-) α -HCH gave a primary KIE_C of 1.0169 (C-H) and 1.0104 (C-Cl).³⁸ The calculated primary
290 KIE_C of (-) α -HCH was smaller than (+) α -HCH during dehydrochlorination, which is in
291 agreement with the observations in our experiments. The AKIE_C of (-) α -HCH in our study is
292 consistent within an order of magnitude with values obtained for quantum mechanical
293 modeling.³⁸ The AKIE_C of (+) α -HCH degradation is higher than the value obtained from
294 quantum chemical modeling but similar with values observed in other studies which report C-Cl
295 bond cleavage at a sigma hybridized carbon.³⁸⁻⁴⁰

296 Assuming that the dehydrochlorination mechanism for both enantiomers is identical and follows
297 E2 elimination,³⁷ the rate limitation might be the result of HCH binding within the enzyme
298 pocket. Binding of γ and β substrates within LinA can affect the transition state and the reaction
299 rates as suggested by QM/MM modeling studies.³⁷ Preceding reaction steps such as transport in
300 the cell and binding to the enzyme can modify the kinetic isotope effect (KIE) of the bond
301 cleavage reaction.⁴¹ As the chemical bond cleavage is probably not much different in a chemical
302 sense, one may hypothesize that the kinetics of the binding to enzymes leads to rate limitation
303 and thus modifies the observed carbon isotope fractionation. Based on our data, we cannot

304 provide a more detailed evaluation of the rate limitation and carbon isotope fractionation.
305 Further QM/MM modeling studies using a model with complete enzyme structures would be
306 required to solve this question.

307 Enantiomer fractionation can be influenced by two factors: (i) Binding of the substrate to the
308 enzyme with respect to the stereochemical position in the enzyme pocket which can lead to
309 different reaction ratios.⁴² (ii) The reactivity of two individual enzymes with specificity towards
310 enantiomers as observed in the enzyme assays with LinA1 and LinA2. In the second case, the
311 enantiomer degradation should be rationalized as individual substances which are controlled by
312 the expression and activity of individual enzymes within the machinery of the cell.⁴³ However if
313 the kinetic reaction rate is changed due to individual regulation of the individual enzymes, the
314 enantiomer fractionation process cannot be described by a single factor. Indeed, the variability
315 of enantiomer preference observed in experiments with growing cells indicates changes in the
316 abundance and reactivity of the LinA1 and LinA2 enzymes during growth.

317 From the discussion based on the mechanisms of enantiomer and isotope fractionation, we can
318 conclude that these two processes can take place but do not have to be synchronous during the
319 biodegradation of α -HCH. These processes are independent as two different enzymes are
320 involved and depend on the activity of the enzymes. Further discussion based on the effect of
321 mass transport and degradation rates can confirm that enantiomer and isotope fractionations are
322 two independent processes.

323 **Effect of Mass Transport on Isotope and Enantiomer Fractionation.** In order to evaluate the
324 effect of mass transport into the cells, isotope fractionation of α -HCH during experiments with
325 cell suspensions and crude extracts were compared. The isotope effects comparing the cell
326 suspension and crude extract experiments were similar when considering the uncertainty. For
327 (+) α -HCH, with the same κ^+ ($0.12 \pm 0.02 \text{ h}^{-1}$; Table 1), the ϵ_c^+ values obtained from cell
328 suspension (experiment c: $-6.1 \pm 1.1\%$; Table 1) and crude extracts (experiment f: $-8.0 \pm 1.3\%$;
329 Table 1) show that mass transfer across the outer and cytoplasmic membranes may reduce the
330 observed isotope fractionation, leading to a relatively smaller ϵ_c^+ in the cell suspension

331 experiments. Compared to the α -HCH degradation by cell suspension and crude extracts,
332 significant higher ϵ_c^+ values (experiment l and m: $-11.3 \pm 2.0\%$ and $-10.9 \pm 1.5\%$, respectively;
333 Table 1) were obtained in the purified LinA1 experiments. The difference of carbon isotope
334 fractionation between crude extracts and enzyme indicates that cell material such as vesicles or
335 membrane remnants may affect the transport of substrate leading to lower isotope fractionation.
336 Interestingly, ϵ_c^- values obtained from the cell suspension experiments (experiment c and d: $-$
337 $2.3 \pm 0.4\%$ and $-2.3 \pm 0.3\%$; table 1) were only slightly lower than the ones from the crude
338 extracts experiments (experiment g and h: $-3.4 \pm 0.5\%$ and $-3.4 \pm 0.6\%$; table 1). This indicates
339 that mass transfer into the cells does not affect the isotope fractionation of $(-)\alpha$ -HCH
340 significantly. Statistically similar values were also obtained when comparing the pure enzyme
341 and crude extracts experiments, indicating that mass transfer is not limited and that bond
342 cleavage of the reaction governs the observed isotope fractionation.

343 Overall, the uptake and passage through the cell wall lead to rate limitation reducing the carbon
344 isotope fractionation for both enantiomers, which indicates that uptake affects the isotope
345 fractionation of individual enantiomers in a similar way. A similar effect on the reduction of
346 carbon isotope fractionation had been observed with non-enantiomeric substances such as
347 chlorinated ethenes and uptake of substrate into the cell often reduced isotope fractionation.⁴⁴
348 The investigation of enantiomer and isotope fractionation of phenoxypropionic acid herbicides
349 in aerobic biodegradation gave contrasting results as high enantiomer fractionation and minor
350 carbon isotope fractionation were observed.⁴ Qiu and colleagues observed higher carbon isotope
351 fractionation of (R)-DCPP in RdpA enzyme degradation compared to degradation by the whole
352 cell of the host organism.⁴ However, the enantiomer fractionation during uptake was not studied
353 in detail. They speculated on active transport over the cell membrane as a mechanism of
354 enantiomer fractionation and masking of isotope fractionation. In contrast, the enantiomer and
355 isotope fractionation during α -HCH degradation are related to the reaction kinetics which is
356 governed by the uptake into the cell and activity of individual enzymes.

357 The mass transport into cells and within the cells is a rate limiting step prior to isotope sensitive
358 bond cleavage and reduces the isotope fractionation of (+) α - and (-) α -HCH leading in both cases
359 to smaller ϵ_c . The ES values of cell suspensions with uptake through the cell membrane
360 (experiment b-d) averages to -0.45 ± 0.03 and crude extracts without membrane passage averages
361 to -0.60 ± 0.05 , suggesting that the rate limitations of the reaction caused by membrane transport
362 are similar to masking of isotope fractionation. However, as enantiomer fractionation depends
363 on the different degradation rates of (-) and (+) α -HCH, it can be changed if the degradation of
364 both enantiomers are affected to a different extent by mass transfer limitation. Comparing to the
365 cell suspension experiments, the relatively higher ES values in the crude extracts experiments
366 indicate that the membrane affects the uptake of the individual enantiomers into the cells at
367 different extents (κ^+/κ^- is not constant throughout the degradation) and lead to the different ES
368 values.

369 **Effect of Degradation Rate on Isotope and Enantiomer Fractionation.** For (-) α -HCH
370 degradation, significant carbon isotope fractionation of (-) α -HCH in the cell suspension
371 experiments was only observed when the κ^- were $0.35 \pm 0.02 \text{ h}^{-1}$ and $0.15 \pm 0.02 \text{ h}^{-1}$. Higher κ^-
372 values (experiment a and b: 0.81 ± 0.12 and $0.76 \pm 0.09 \text{ h}^{-1}$) led to lower or even disappearance of
373 isotope fractionation. In crude extract experiments, the relatively higher κ^- of experiment f
374 ($0.45 \pm 0.06 \text{ h}^{-1}$) led to lower ϵ_c^- compared to experiment g and h. In both cell suspension and
375 crude extract experiments, it is demonstrated that isotope fractionation at higher rates does not
376 characterize the bond cleavage because it is not the rate determining step of the reaction in (-) α -
377 HCH degradation. In the case of (+) α -HCH degradation, when the κ^+ value of cell suspension
378 experiments fall below 0.5 h^{-1} , significant isotope fractionation can be observed and the ϵ_c of
379 (+) α -HCH was nearly identical in parallel experiments (Table 1). The same results were
380 observed in the crude extracts experiments. In this case, the degradation rate did not
381 significantly affect the carbon isotope fractionation of (+) α -HCH and the bond cleavage was the
382 main rate limiting step of the reaction.

383 The ES values indicate preferential degradation of (-) α -HCH over (+) α -HCH in all cell
384 suspension and crude extract experiments. Comparison of ES values from cell suspensions
385 (avg.= -0.45 ± 0.03) with crude extracts (avg.= -0.60 ± 0.05) suggests that uptake into the cells
386 reduced the enantiomer fractionation to some extent. As diffusion is identical for enantiomers,
387 the passive chemical passage through the membrane should not affect the enantiomer
388 composition.

389 Therefore, the degradation kinetics of both enantiomers governs enantiomer fractionation and it
390 will be constant if the degradation kinetics of both enantiomers is affected to the same extent.
391 This is mechanistically not comparable to mass transfer limitations that affect isotope
392 fractionation, as two individual substances are catalyzed by two enzymes and the variability of
393 the degradation rates does not allow for a correlation with independent mass transfer limitations.

394 **ENVIRONMENTAL IMPLICATION**

395 Transformation of α -HCH by LinA1 and LinA2 enzymes exhibits a pronounced specificity for
396 (+) α -HCH and (-) α -HCH, respectively. Therefore, the extent of aerobic degradation of α -HCH
397 in field sites can be quantified robustly by enantiomer-specific stable isotope analysis.
398 Additionally, the reported ϵ_C values can be used for evaluation of aerobic α -HCH enantiomer
399 degradation in field sites. The variable enantiomer preference during α -HCH degradation by
400 *Sphingobium* spp. under growth conditions indicates the challenge of applying enantiomer
401 fractionation for quantification. Variable enantiomer fractionation leads to uncertainty for
402 quantitative work. However, compared to the nutrient rich culture medium, the microbes in field
403 sites can be limited by various abiotic and biotic factors, such as energy sources, levels of
404 oxygen, temperatures, pH and osmolality.⁴⁵ Consequently, the growth of bacteria may be
405 relatively slower (due to limitations of temperature, nutrients etc.) leading to a slower renewal
406 and expression of enzymes. In this case, the inventory of enzymes may not change quickly
407 leading to stable enantiomer preference as proved in our degradation experiment under nutrient-

408 limited condition. Therefore, the enantiomer fractionation might be applied for quantification of
409 enantiomer degradation in field site.

410 In a recent paper, we used isotope fractionation of individual α -HCH enantiomers and
411 enantiomer fractionation for characterizing *in situ* biodegradation in complex aquifer systems in
412 Bitterfeld, Germany, with changing hydrological conditions.⁴⁶ The results showed discrepancies
413 in the extent of biodegradation calculated by Rayleigh equation based on isotope and
414 enantiomer fractionation. The quantification of enantiomer fractionation using the Rayleigh
415 concepts is mathematically inconsistent which leads to uncertainty. For quantification of
416 enantiomer fractionation, the ES, instead of enantiomer fractionation factor based on Rayleigh
417 equation, should be determined. ES is mathematically consistent as long as the degradation of
418 enantiomers can be described by the first order kinetics. However, the study presented here on
419 ES and CSIA of enantiomers showed that ES is variable and depends on growth conditions.
420 Hence, ES needs to be used with reservation for quantitative work. Nevertheless, the
421 combination of isotope fractionation and enantiomer fractionation for field site evaluation can
422 take advantage of enantiomer fractionation for characterizing aerobic degradation processes
423 qualitatively and help to select a fractionation factor for quantifying biodegradation. Thus, this
424 study represents the first step towards developing a better understanding of isotope and
425 enantiomer fractionation and will aid in field site evaluation.

426 **AUTHOR INFORMATION**

427 Corresponding Author: Hans-Hermann Richnow

428 Phone: +49-3412351212; Fax: +49-341450822; E-mail: hans.richnow@ufz.de

429 **ACKNOWLEDGEMENTS**

430 We acknowledge the financial support from the German-Israeli Foundation for Research and
431 Development (GIF) Grant no. I-1368-307.8/2016 (“Prediction of chiral and isotope enrichment
432 during the transformations of halo-organic pollutants: Mechanistic and QSAR approaches”). We

433 are grateful for the fellowship of Yaqing Liu (File No. 201301542002) and Langping Wu (File
434 No. 201306460007) from the China Scholarship Council. Jia Liu is acknowledged for her
435 support during set up fractionation experiments, extraction and enzyme experiments. M. Gehre,
436 S. Kümmel and U. Günther are acknowledged for continuous analytical support in the Isotope
437 Laboratory of the Department of Isotope Biogeochemistry. We acknowledge the financial
438 support of The German Academic Exchange Service (DAAD) and The Department of Science
439 & Technology (DST) in the personal exchange program DAAD project 57035944 and DST
440 project INT/FRG/DAAD/P-231/2013 for funding travel expenses, particularly for Puneet Kohli
441 and Roshan Kumar. We thank for critical comments of all the anonymous reviewers and the
442 editor, particularly for the quantification of enantiomer fractionation.

443 **Supporting Information**

444 Details on strain cultivation, experimental conductions, analytic methods and summary of
445 observed data can be found in supporting information.

446 **REFERENCE**

- 447 1. Ye, J.; Zhao, M.; Niu, L.; Liu, W., Enantioselective environmental toxicology of chiral
448 pesticides. *Chem. Res. Toxicol.* **2015**, *28*, (3), 325-38.
- 449 2. Burden, R. S.; Carter, G. A.; Clark, T.; Cooke, D. T.; Croker, S. J.; Deas, A. H.; Hedden,
450 P.; James, C. S.; Lenton, J. R., Comparative activity of the enantiomers of triadimenol and
451 paclobutrazol as inhibitors of fungal growth and plant sterol and gibberellin biosynthesis. *Pest.*
452 *Manag. Sci.* **1987**, *21*, (4), 253-267.
- 453 3. Wong, C. S., Environmental fate processes and biochemical transformations of chiral
454 emerging organic pollutants. *Anal. Bioanal. Chem.* **2006**, *386*, (3), 544-558.
- 455 4. Qiu, S.; Gözdereliler, E.; Weyrauch, P.; Lopez, E. C. M.; Kohler, H.-P. E.; Sørensen, S.
456 R.; Meckenstock, R. U.; Elsner, M., Small $^{13}\text{C}/^{12}\text{C}$ Fractionation Contrasts with Large
457 Enantiomer Fractionation in Aerobic Biodegradation of Phenoxy Acids. *Environ. Sci. Technol.*
458 **2014**, *48*, (10), 5501-5511.
- 459 5. Muller, T. A.; Kohler, H. P., Chirality of pollutants--effects on metabolism and fate.
460 *Appl. Microbiol. Biotechnol.* **2004**, *64*, (3), 300-16.
- 461 6. Hashim, N.; Shafie, S.; Khan, S., Enantiomeric fraction as an indicator of
462 pharmaceutical biotransformation during wastewater treatment and in the environment--a
463 review. *Environ. Technol.* **2010**, *31*, (12), 1349-1370.
- 464 7. Nijenhuis, I.; Richnow, H. H., Stable isotope fractionation concepts for characterizing
465 biotransformation of organohalides. *Curr. Opin. Biotechnol.* **2016**, *41*, 108-113.

- 466 8. Vogt, C.; Dorer, C.; Musat, F.; Richnow, H.-H., Multi-element isotope fractionation
467 concepts to characterize the biodegradation of hydrocarbons—from enzymes to the
468 environment. *Curr. Opin. Biotechnol.* **2016**, *41*, 90-98.
- 469 9. Elsner, M.; Jochmann, M. A.; Hofstetter, T. B.; Hunkeler, D.; Bernstein, A.; Schmidt, T.
470 C.; Schimmelmann, A., Current challenges in compound-specific stable isotope analysis of
471 environmental organic contaminants. *Anal. Bioanal. Chem.* **2012**, *403*, (9), 2471-2491.
- 472 10. Nijenhuis, I.; Renpenning, J.; Kümmel, S.; Richnow, H. H.; Gehre, M., Recent advances
473 in multi-element compound-specific stable isotope analysis of organohalides: Achievements,
474 challenges and prospects for assessing environmental sources and transformation. *Trends*
475 *Environ. Anal. Chem.* **2016**, *11*, 1-8.
- 476 11. Gasser, G.; Pankratov, I.; Elhanany, S.; Werner, P.; Gun, J.; Gelman, F.; Lev, O., Field
477 and laboratory studies of the fate and enantiomeric enrichment of venlafaxine and O-
478 desmethylvenlafaxine under aerobic and anaerobic conditions. *Chemosphere* **2012**, *88*, (1), 98-
479 105.
- 480 12. Bashir, S.; Fischer, A.; Nijenhuis, I.; Richnow, H. H., Enantioselective carbon stable
481 isotope fractionation of hexachlorocyclohexane during aerobic biodegradation by *Sphingobium*
482 spp. *Environ. Sci. Technol.* **2013**, *47*, (20), 11432-11439.
- 483 13. Jammer, S.; Voloshenko, A.; Gelman, F.; Lev, O., Chiral and isotope analyses for
484 assessing the degradation of organic contaminants in the environment: Rayleigh dependence.
485 *Environ. Sci. Technol.* **2014**, *48*, (6), 3310-3318.
- 486 14. Ivdra, N.; Fischer, A.; Herrero-Martin, S.; Giunta, T.; Bonifacie, M.; Richnow, H.-H.,
487 Carbon, Hydrogen and Chlorine Stable Isotope Fingerprinting for Forensic Investigations of
488 Hexachlorocyclohexanes. *Environ. Sci. Technol.* **2016**, *51*, (1), 446-454.
- 489 15. Nagata, Y.; Miyauchi, K.; Takagi, M., Complete analysis of genes and enzymes for γ -
490 hexachlorocyclohexane degradation in *Sphingomonas paucimobilis* UT26. *J. Ind. Microbiol.*
491 *Biotechnol.* **1999**, *23*, (4), 380-390.
- 492 16. Kumari, R.; Subudhi, S.; Suar, M.; Dhingra, G.; Raina, V.; Dogra, C.; Lal, S.; van der
493 Meer, J. R.; Holliger, C.; Lal, R., Cloning and characterization of lin genes responsible for the
494 degradation of hexachlorocyclohexane isomers by *Sphingomonas paucimobilis* strain B90. *Appl.*
495 *Environ. Microb.* **2002**, *68*, (12), 6021-6028.
- 496 17. Lal, R.; Pandey, G.; Sharma, P.; Kumari, K.; Malhotra, S.; Pandey, R.; Raina, V.;
497 Kohler, H. P.; Holliger, C.; Jackson, C.; Oakeshott, J. G., Biochemistry of microbial degradation
498 of hexachlorocyclohexane and prospects for bioremediation. *Microbiol. Mol. Biol. Rev.* **2010**,
499 *74*, (1), 58-80.
- 500 18. Böltner, D.; Moreno - Morillas, S.; Ramos, J. L., 16S rDNA phylogeny and distribution
501 of lin genes in novel hexachlorocyclohexane - degrading *Sphingomonas* strains. *Environ.*
502 *Microbiol.* **2005**, *7*, (9), 1329-1338.
- 503 19. Mohn, W. W.; Mertens, B.; Neufeld, J. D.; Verstraete, W.; de Lorenzo, V., Distribution
504 and phylogeny of hexachlorocyclohexane-degrading bacteria in soils from Spain. *Environ*
505 *Microbiol* **2006**, *8*, (1), 60-8.
- 506 20. Sharma, P.; Pandey, R.; Kumari, K.; Pandey, G.; Jackson, C. J.; Russell, R. J.;
507 Oakeshott, J. G.; Lal, R., Kinetic and sequence-structure-function analysis of known LinA
508 variants with different hexachlorocyclohexane isomers. *PLoS One* **2011**, *6*, (9), e25128.
509 doi:10.1371/journal.pone.0025128
- 510 21. Shrivastava, N.; Macwan, A. S.; Kohler, H. E.; Kumar, A., Important amino acid
511 residues of hexachlorocyclohexane dehydrochlorinases (LinA) for enantioselective
512 transformation of hexachlorocyclohexane isomers. *Biodegradation* **2017**, *28*, (2-3), 171-180.
- 513 22. Macwan, A. S.; Kukshal, V.; Srivastava, N.; Javed, S.; Kumar, A.; Ramachandran, R.,
514 Crystal structure of the hexachlorocyclohexane dehydrochlorinase (LinA-type2): mutational
515 analysis, thermostability and enantioselectivity. *PLoS One* **2012**, *7*, (11), e50373.
516 doi:10.1371/journal.pone.0050373
- 517 23. Pal, R.; Bala, S.; Dadhwal, M.; Kumar, M.; Dhingra, G.; Prakash, O.; Prabakaran, S. R.;
518 Shivaji, S.; Cullum, J.; Holliger, C.; Lal, R., Hexachlorocyclohexane-degrading bacterial strains

519 *Sphingomonas paucimobilis* B90A, UT26 and Sp+, having similar lin genes, represent three
520 distinct species, *Sphingobium indicum* sp. nov., *Sphingobium japonicum* sp. nov. and
521 *Sphingobium francense* sp. nov., and reclassification of [*Sphingomonas*] chungbukensis as
522 *Sphingobium chungbukense* comb. nov. *Int. J. Syst. Evol. Microbiol.* **2005**, *55*, (Pt 5), 1965-72.

523 24. Singh, A. K.; Chaudhary, P.; Macwan, A. S.; Diwedi, U. N.; Kumar, A., Selective loss
524 of lin genes from hexachlorocyclohexane-degrading *Pseudomonas aeruginosa* ITRC-5 under
525 different growth conditions. *Appl. Microbiol. Biotechnol.* **2007**, *76*, (4), 895-901.

526 25. Suar, M.; van der Meer, J. R.; Lawlor, K.; Holliger, C.; Lal, R., Dynamics of multiple lin
527 gene expression in *Sphingomonas paucimobilis* B90A in response to different
528 hexachlorocyclohexane isomers. *Appl. Environ. Microbiol.* **2004**, *70*, (11), 6650-6.

529 26. Verma, H.; Kumar, R.; Oldach, P.; Sangwan, N.; Khurana, J. P.; Gilbert, J. A.; Lal, R.,
530 Comparative genomic analysis of nine *Sphingobium* strains: insights into their evolution and
531 hexachlorocyclohexane (HCH) degradation pathways. *BMC genomics* **2014**, *15*, (1), 1014.
532 doi:10.1186/1471-2164-15-1014

533 27. Bashir, S.; Fischer, A.; Nijenhuis, I.; Richnow, H. H., Enantioselective carbon stable
534 isotope fractionation of hexachlorocyclohexane during aerobic biodegradation by *Sphingobium*
535 spp. *Environ. Sci. Technol.* **2013**, *47*, (20), 11432-9.

536 28. Badea, S. L.; Vogt, C.; Gehre, M.; Fischer, A.; Danet, A. F.; Richnow, H. H.,
537 Development of an enantiomer-specific stable carbon isotope analysis (ESIA) method for
538 assessing the fate of alpha-hexachlorocyclo-hexane in the environment. *Rapid Commun. Mass.*
539 *Sp.* **2011**, *25*, (10), 1363-1372.

540 29. Schilling, I. E.; Bopp, C. E.; Lal, R.; Kohler, H. E.; Hofstetter, T. B., Assessing Aerobic
541 Biotransformation of Hexachlorocyclohexane Isomers by Compound-Specific Isotope Analysis.
542 *Environ. Sci. Technol.* **2019**, *53*, (5), 2353-2363.

543 30. Mueller, M. D.; Buser, H.-R., Environmental Behavior of Acetamide Pesticide
544 Stereoisomers. 2. Stereo- and Enantioselective Degradation in Sewage Sludge and Soil.
545 *Environ. Sci. Technol.* **1995**, *29*, (8), 2031-2037.

546 31. Buerge, I. J.; Poiger, T.; Müller, M. D.; Buser, H.-R., Enantioselective Degradation of
547 Metalaxyl in Soils: Chiral Preference Changes with Soil pH. *Environ. Sci. Technol.* **2003**, *37*,
548 (12), 2668-2674.

549 32. Suar, M.; Hauser, A.; Poiger, T.; Buser, H. R.; Muller, M. D.; Dogra, C.; Raina, V.;
550 Holliger, C.; van der Meer, J. R.; Lal, R.; Kohler, H. P., Enantioselective transformation of
551 alpha-hexachlorocyclohexane by the dehydrochlorinases LinA1 and LinA2 from the soil
552 bacterium *Sphingomonas paucimobilis* B90A. *Appl. Environ. Microb.* **2005**, *71*, (12), 8514-
553 8518.

554 33. Elsner, M.; Zwank, L.; Hunkeler, D.; Schwarzenbach, R. P., A new concept linking
555 observable stable isotope fractionation to transformation pathways of organic pollutants.
556 *Environ. Sci. Technol.* **2005**, *39*, (18), 6896-6916.

557 34. Northrop, D. B., The expression of isotope effects on enzyme-catalyzed reactions. *Annu.*
558 *Rev. Biochem.* **1981**, *50*, (1), 103-131.

559 35. Swiderek, K.; Paneth, P., Binding isotope effects. *Chem. Rev.* **2013**, *113*, (10), 7851-79.

560 36. Okai, M.; Kubota, K.; Fukuda, M.; Nagata, Y.; Nagata, K.; Tanokura, M., Crystal
561 structure of gamma-hexachlorocyclohexane Dehydrochlorinase LinA from *Sphingobium*
562 *japonicum* UT26. *J. Mol. Biol.* **2010**, *403*, (2), 260-9.

563 37. Manna, R. N.; Zinovjev, K.; Tunon, I.; Dybala-Defratyka, A., Dehydrochlorination of
564 Hexachlorocyclohexanes Catalyzed by the LinA Dehydrohalogenase. A QM/MM Study. *J.*
565 *Phys. Chem. B* **2015**, *119*, (49), 15100-9.

566 38. Manna, R. N.; Dybala-Defratyka, A., Insights into the elimination mechanisms
567 employed for the degradation of different hexachlorocyclohexane isomers using kinetic isotope
568 effects and docking studies. *J. Phys. Org. Chem.* **2013**, *26*, (10), 797-804.

569 39. Nikolausz, M.; Nijenhuis, I.; Ziller, K.; Richnow, H. H.; Kästner, M., Stable carbon
570 isotope fractionation during degradation of dichloromethane by methylotrophic bacteria.
571 *Environ. Microbiol.* **2006**, *8*, (1), 156-164.

- 572 40. Fletcher, K. E.; Löffler, F. E.; Richnow, H.-H.; Nijenhuis, I., Stable carbon isotope
573 fractionation of 1, 2-dichloropropane during dichloroelimination by *Dehalococcoides*
574 populations. *Environ. Sci. Technol.* **2009**, *43*, (18), 6915-6919.
- 575 41. Nijenhuis, I.; Andert, J.; Beck, K.; Kastner, M.; Diekert, G.; Richnow, H. H., Stable
576 isotope fractionation of tetrachloroethene during reductive dechlorination by *Sulfurospirillum*
577 *multivorans* and *Desulfitobacterium* sp. strain PCE-S and abiotic reactions with
578 cyanocobalamin. *Appl. Environ. Microb.* **2005**, *71*, (7), 3413-9.
- 579 42. Reetz, M. T., Laboratory evolution of stereoselective enzymes: a prolific source of
580 catalysts for asymmetric reactions. *Angew. Chem. Int. Ed.* **2011**, *50*, (1), 138-174.
- 581 43. Muller, R. H.; Kleinstüber, S.; Babel, W., Physiological and genetic characteristics of
582 two bacterial strains utilizing phenoxypropionate and phenoxyacetate herbicides. *Microbiol.*
583 *Res.* **2001**, *156*, (2), 121-31.
- 584 44. Renpenning, J.; Rapp, I.; Nijenhuis, I., Substrate hydrophobicity and cell composition
585 influence the extent of rate limitation and masking of isotope fractionation during microbial
586 reductive dehalogenation of chlorinated ethenes. *Environ. Sci. Technol.* **2015**, *49*, (7), 4293-301.
- 587 45. van Elsas, J. D.; Semenov, A. V.; Costa, R.; Trevors, J. T., Survival of *Escherichia coli*
588 in the environment: fundamental and public health aspects. *ISME J.* **2011**, *5*, (2), 173-83.
- 589 46. Liu, Y.; Bashir, S.; Stollberg, R.; Trabitsh, R.; Weiss, H.; Paschke, H.; Nijenhuis, I.;
590 Richnow, H. H., Compound Specific and Enantioselective Stable Isotope Analysis as Tools To
591 Monitor Transformation of Hexachlorocyclohexane (HCH) in a Complex Aquifer System.
592 *Environ. Sci. Technol.* **2017**, *51*, (16), 8909-8916.
593

594 **Tables and figures**

595 Table 1. Summary of stable carbon isotope enrichment factors (ϵ_c), enantioselectivity (ES), and related kinetic rate constants (κ) in different sets of α -
 596 HCH degradation experiments by cell suspension, crude extracts and LinA enzymes of strain B90A.

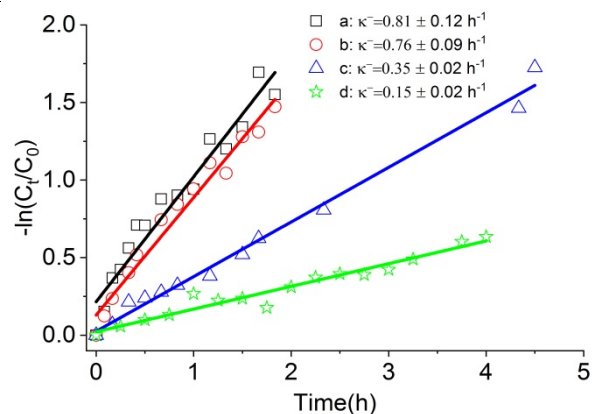
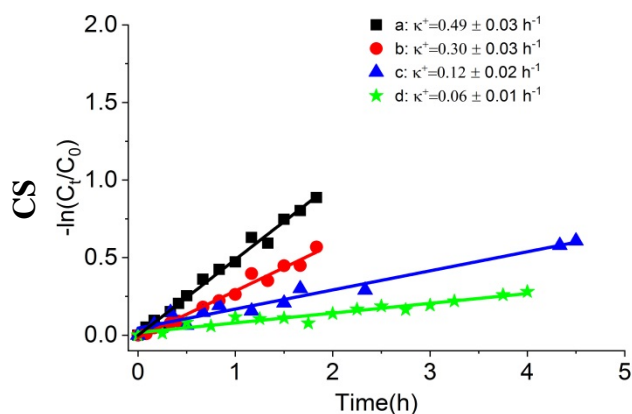
	M	N	Amount of biomass (μ L)	Kinetic constant				Isotope fractionation				Enantiomer fractionation	
				(-) α -HCH		(+) α -HCH		(-) α -HCH		(+) α -HCH		ES	
			$\kappa^- \pm \text{CI}_{95\%}$ (h^{-1})	R^2	$\kappa^+ \pm \text{CI}_{95\%}$ (h^{-1})	R^2	$\epsilon_c^- \pm \text{CI}_{95\%}$ (‰)	R^2	$\epsilon_c^+ \pm \text{CI}_{95\%}$ (‰)	R^2			
cell suspension	a	15	300	0.81±0.12	0.95	0.49±0.03	0.99	n.s.	n.s.	-6.4±0.7	0.97	-0.25±0.08	
	b	13	200	0.76±0.09	0.97	0.30±0.03	0.98	n.s.	n.s.	-6.2±1.2	0.92	-0.43±0.06	
	c	12	100	0.35±0.02	0.99	0.12±0.02	0.96	-2.3±0.4	0.92	-6.1±1.1	0.93	-0.49±0.07	avg.= -0.45±0.03
	d	16	50	0.15±0.02	0.95	0.06±0.01	0.93	-2.3±0.3	0.95	-6.1±1.4	0.87	-0.43±0.09	
									avg.= -2.3; sd.=0.03		avg.= -6.2; sd.=0.1		
Crude extracts	e	10	200	0.58±0.13	0.94	0.30±0.07	0.93	n.s.	n.s.	-7.4±0.7	0.99	-0.32±0.15	
	f	13	100	0.45±0.06	0.96	0.12±0.02	0.91	-1.9±0.4	0.90	-8.0±1.3	0.94	-0.58±0.07	
	g	13	50	0.19±0.02	0.98	0.04±0.01	0.95	-3.4±0.5	0.96	n.a.	n.a.	-0.65±0.08	avg.= -0.60±0.05
	h	14	50	0.18±0.04	0.91	0.05±0.01	0.91	-3.4±0.6	0.92	n.a.	n.a.	-0.57±0.10	
									avg.= -3.4; sd.=0.02		avg.= -7.7; sd.=0.4		
LinA2	i	13	10	0.65±0.10	0.95	n.a.	n.a.	-3.7±0.6	0.95	n.a.	n.a.	-1	
	j	9	8	0.54±0.28	0.74	n.a.	n.a.	-4.0±1.0	0.93	n.a.	n.a.	-1	
	k	14	5	0.27±0.05	0.91	n.a.	n.a.	-3.6±0.5	0.95	n.a.	n.a.	-1	
									avg.= -3.8; sd.=0.2				
LinA1	l	13	10	n.a.	n.a.	0.28±0.02	0.98	n.a.	n.a.	-11.3±2.0	0.94	1	
	m	14	5	n.a.	n.a.	0.13±0.02	0.93	n.a.	n.a.	-10.9±1.5	0.96	1	
										avg.= -11.1; sd.= 0.3			

597
 598 M: different sets of the experiments and the detailed experimental conditions can be found in the Experimental Section; N: number of samples; $\text{CI}_{95\%}$:
 599 Confidence interval at level 95%; n.a.: not assessed since degradation was negligible; n.s.: degradation observed but no significant or no consistent
 600 isotope enrichment was observed, the detail information are reported in SI7); avg.: average value; sd.: standard deviation.

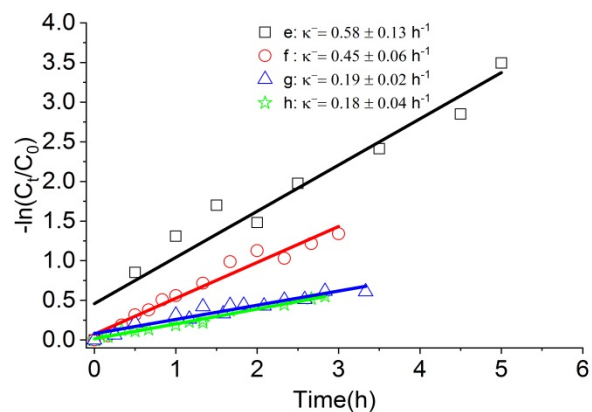
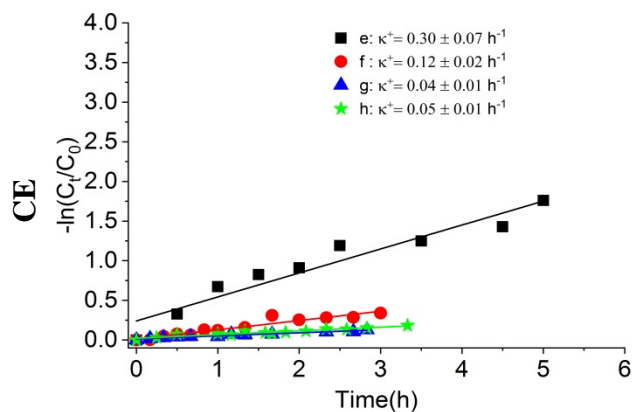
601

(+)α-HCH**(-)α-HCH**

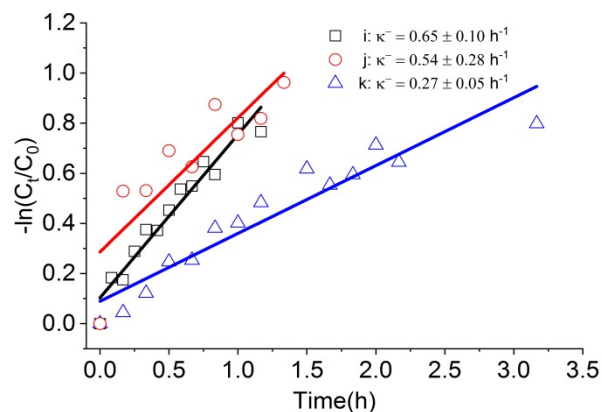
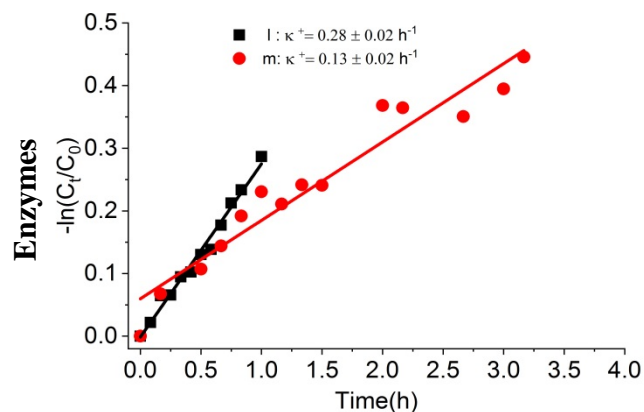
602



603



604



605

606 Figure 1. The degradation kinetics of (+)α-HCH (close symbols) and (-)α-HCH (open symbols)
 607 by cell suspension (CS) and crude extracts (CE) of *S. indicum* strain B90A and the
 608 corresponding enzymes (LinA1 and LinA2). The letter a-k represents different experimental
 609 conditions that are defined in the experimental section

610

611

612

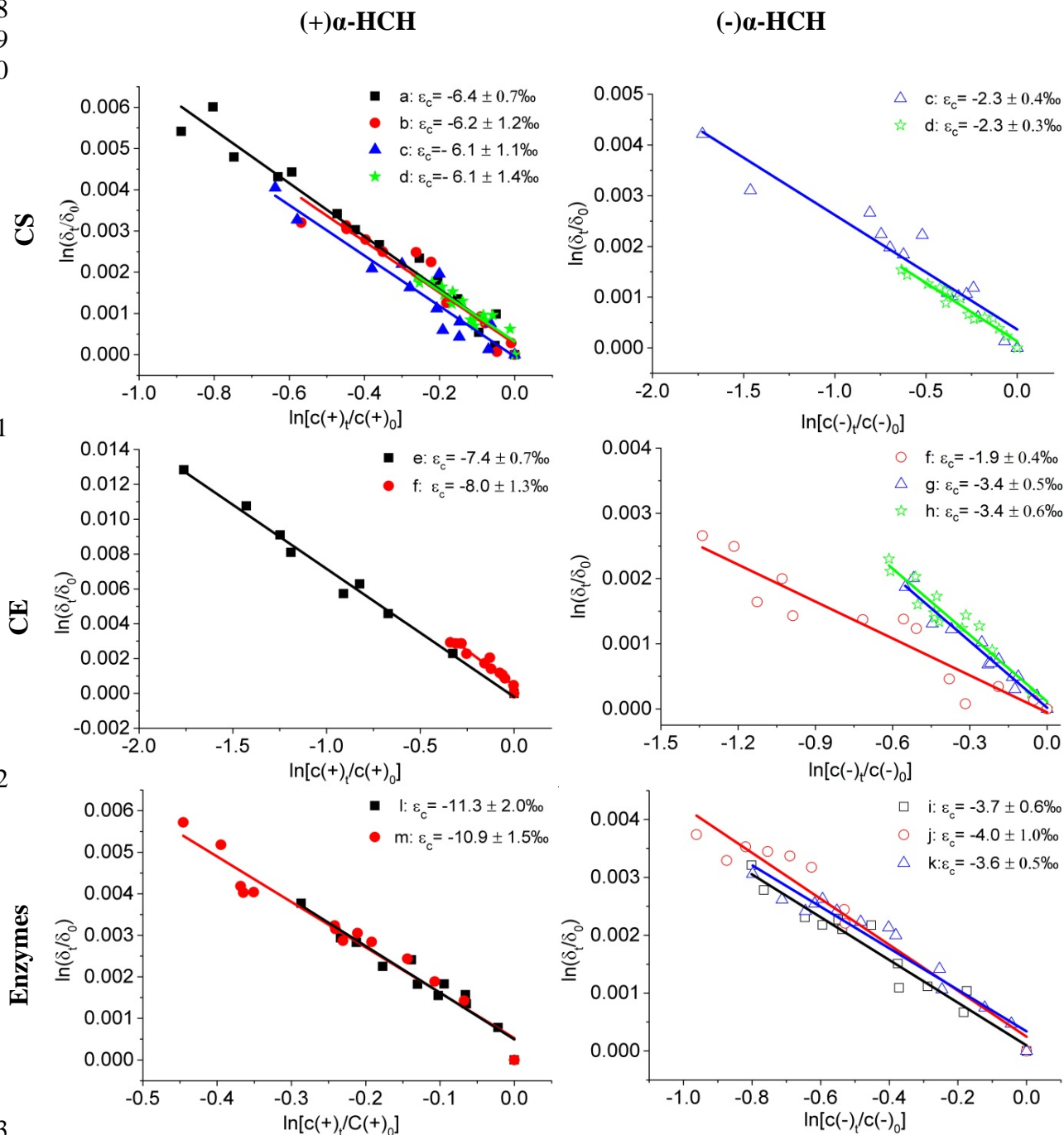
613

614

615
616
617
618
619
620

621

622



623

624 Figure 2. Linearized Rayleigh equation plots showing the carbon isotope fractionation for the
625 biodegradation of α -HCH enantiomers (close symbols for (+) α -HCH and open symbols for (-) α -
626 HCH) by cell suspension (CS) and crude extracts (CE) of *S. indicum* strain B90A and the
627 corresponding enzymes LinA1 and LinA2. The individual evaluation of the isotope fractionation
628 for each experiment can be found in Figure S8 (CS), Figure S9 (CE), Figure S10 (LinA2) and
629 Figure S111 (LinA1). The letter a-k represents different experimental conditions that are defined
630 in the experimental section and summarized in Table 1.

631